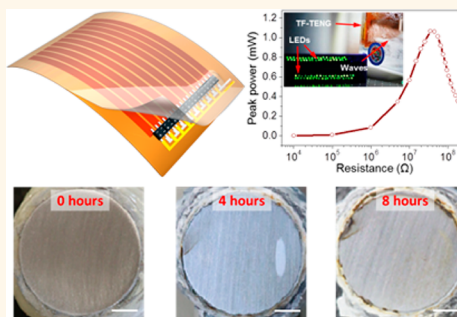


Triboelectric Charging at the Nanostructured Solid/Liquid Interface for Area-Scalable Wave Energy Conversion and Its Use in Corrosion Protection

Xue Jiao Zhao,^{†,§} Guang Zhu,^{*,†,§} You Jun Fan,[†] Hua Yang Li,[†] and Zhong Lin Wang^{†,‡}

[†]Beijing Institute of Nanoenergy and Nanosystems, Chinese Academy of Sciences, Beijing 100083, China and [‡]School of Materials Science and Engineering, Georgia Institute of Technology, Atlanta, Georgia 30332, United States. [§]X.J.Z. and G.Z. contributed equally to this work.

ABSTRACT We report a flexible and area-scalable energy-harvesting technique for converting kinetic wave energy. Triboelectrification as a result of direct interaction between a dynamic wave and a large-area nanostructured solid surface produces an induced current among an array of electrodes. An integration method ensures that the induced current between any pair of electrodes can be constructively added up, which enables significant enhancement in output power and realizes area-scalable integration of electrode arrays. Internal and external factors that affect the electric output are comprehensively discussed. The produced electricity not only drives small electronics but also achieves effective impressed current cathodic protection. This type of thin-film-based device is a potentially practical solution of on-site sustained power supply at either coastal or off-shore sites wherever a dynamic wave is available. Potential applications include corrosion protection, pollution degradation, water desalination, and wireless sensing for marine surveillance.



KEYWORDS: wave energy · energy conversion · contact electrification · triboelectric generator · corrosion protection

Ambient water motions, especially dynamic waves, contain a gigantic reserve of kinetic energy but are hardly utilized in an effective way.^{1–3} Harvesting wave energy not only provides a viable means of producing renewable energy but also opens up a new path to self-powered technology without an external power source.⁴ It can be potentially applied in a variety of circumstances wherever electricity is needed, including corrosion protection, pollution degradation, water desalination, and wireless sensing for marine surveillance.^{5,6} Conventional approaches to harvesting wave energy by using electromagnetic generators have drawbacks of bulky size and heavy weight.^{6–8} In recent years, a novel method for this purpose was developed, which utilized triboelectrification at the solid/liquid interface.^{9–14} A direct and reciprocating interaction between a dynamic wave and a solid surface produces alternating

current flow between a pair of electrodes underneath. Since this approach relies on a surface effect, it is prominent in energy density in terms of power per volume. Furthermore, it does not require additional components for capturing and transferring mechanical motions of the wave, which is a unique advantage compared to other conventional methods.^{15–17} Although this approach showed exciting prospects of harvesting energy from waves, some major challenges are still to be addressed. Foremost, the electric power needs much further improvement. Though it was found in previous reports that fine electrodes are beneficial for enhancing output power density,¹¹ it lacked an effective means of integrating a number of electrodes together to make them area-scalable. Second, nanostructures at the solid/liquid interface that play a key role in promoting the electric power also need to be scaled up in area if this technique

* Address correspondence to zhuguang@binn.cas.cn.

Received for review May 21, 2015 and accepted July 8, 2015.

Published online July 08, 2015
10.1021/acsnano.5b03093

© 2015 American Chemical Society

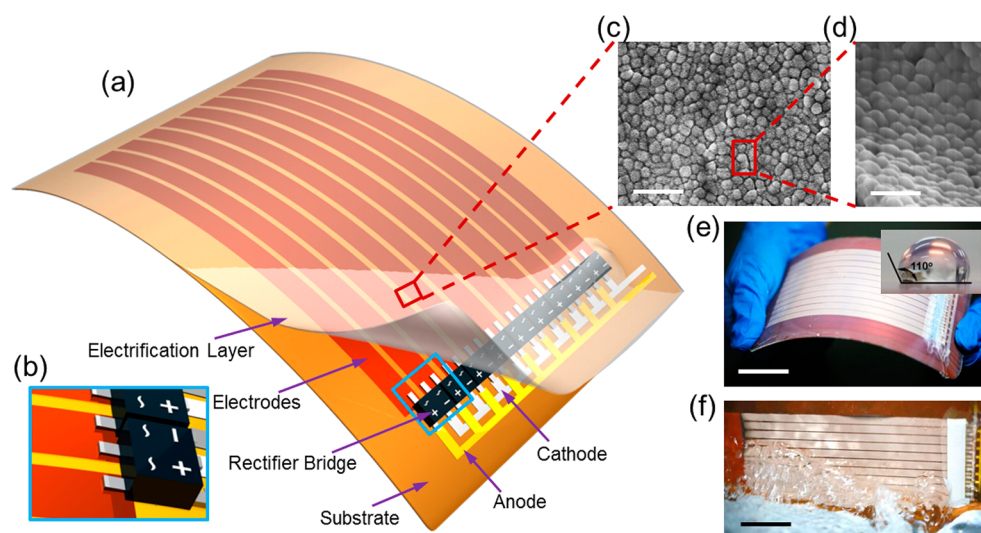


Figure 1. Structure of a thin-film triboelectric generator (TF-TEG). (a) Schematic diagram of an integrated TF-TEG. (b) Enlarged sketch of the arrayed bridge rectifiers. (c) SEM image of the PTFE nanoparticles on the electrification layer (scale bar = 1 μm). (d) Enlarged view of the nanoparticles at a tilted angle of 60° (scale bar = 500 nm). (e) Picture of a bendable as-fabricated TF-TEG. Inset: Water contact angle on the nanostructured surface (scale bar = 25 mm). (f) Picture of the TF-TEG that is interacting with the water wave (scale bar = 25 mm).

is to be practically used. Besides, further applications in addition to powering small electronics are to be demonstrated.

Here, we report a flexible thin-film triboelectric generator (TF-TEG) for harvesting kinetic wave energy. Triboelectric charge at the nanostructured solid/liquid interface induces flow of free electrons in an external circuit as the device has repeated contact with the surrounding water body. An integration approach is developed by using an array of surface-mounted bridge rectifiers to connect multiple parallel electrodes together. As a result, induced charge flow between any pair of adjacent electrodes can be rectified and then constructively added up to form pulsed direct current between an anode and a cathode. Surface nanostructure of close-packed polytetrafluoroethylene (PTFE) nanoparticles in a large area is fabricated through a spin-coating technique, providing an area-scalable route for obtaining high-level electric power. A TF-TEG having lateral dimensions of 100 mm by 60 mm with a total of 11 electrodes can generate an optimum output power of 1.1 mW, which is 10 times that in a previous report.¹¹ The produced electricity not only drives small electronics but also achieves effective impressed current cathodic protection for carbon steel. The corrosion potential of the carbon steel is considerably increased from -111 to -198 mV as the electricity from a TF-TEG is applied. Control experiments exhibit remarkable contrast of surface morphology between the group with protection and the one without. The novel integration approach and the thin-film structure of the TF-TEG bring about a number of unique advantages. It can be conveniently applied onto objects that have direct interaction with waves without considerably adding additional size and weight. As a result, it is a potentially

practical solution of on-site sustained power supply, especially applicable to corrosion protection for coastal constructions, off-shore facilities, and ships where wave energy is abundantly available.

RESULTS AND DISCUSSION

The structure of a TF-TEG is shown in Figure 1a, which is composed of multiple layers. The bottom layer is a flexible 125 μm thick Kapton substrate. A parallel array of strip-shaped copper electrodes (100 mm \times 4.8 mm \times 200 nm for each) is fabricated onto the substrate by mask-assisted sputtering. The interval between adjacent electrodes is 0.7 mm. Bridge rectifiers (4.9 mm \times 4.5 mm \times 1.5 mm) are surface-mounted onto the substrate. As shown in Figure 1b, the two pins at the input side of the rectifiers are connected to a pair of adjacent electrodes with a one-to-one correspondence. Adjacent pins from different rectifiers share the same electrode, as shown in Figure 1b. At the output side, negative pins of all rectifiers are connected together to form a comb-shaped joint cathode, while all positive ones form a joint anode. The cathode and the anode are insulated from each other in regions where they are intersected. The outermost layer is an electrification material made of PTFE thin film (25 μm thick), which is tightly adhered onto the substrate to insulate all components underneath from the surrounding water. PTFE nanoparticles about 200 nm in diameter, shown in the scanning electron microscopy (SEM) images of surface morphology (Figure 1c,d), are densely and uniformly distributed on top of the electrification layer, which plays a key role in promoting the output current. The detailed fabrication process is discussed in the Methods section. The picture of a bent TF-TEG is presented in Figure 1e, which clearly

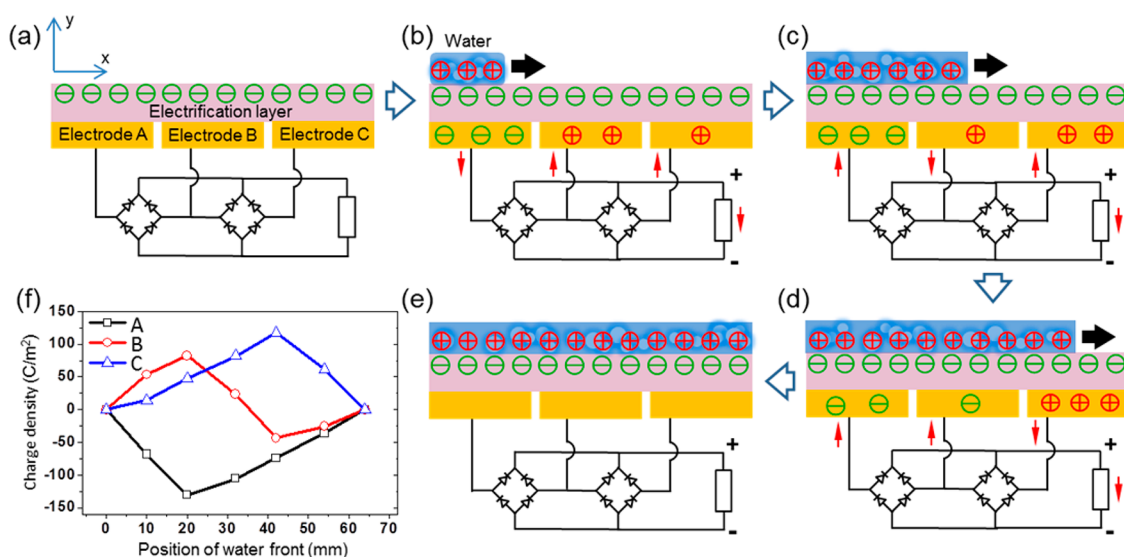


Figure 2. Electricity-generating process of the TF-TEG. (a) Cross-sectional view of charge distribution when the device is fully exposed from water. (b) Charge distribution when water is propagating across electrode A. (c) Charge distribution when water is propagating across electrode B. (d) Charge distribution when water is propagating across electrode C. (e) Charge distribution when water fully covers the electrification layer underneath. (f) Charge density on the three electrodes as the water front propagates.

demonstrates its thin-film structure and flexibility. Due to the hydrophobic nature of the PTFE and the nanoscale surface morphology, the water contact angle of the top surface is 110° (inset of Figure 1e). The good hydrophobicity is important for the generation of an output current, which will be discussed later.

To test the performance of a TF-TEG, it was attached on the side wall of a water tank. A wave generator was used to excite a propagating water wave that repeatedly submerges the TF-TEG, as shown in Figure 1f and movie S1 in the Supporting Information. The electricity generation process of a complete cycle is illustrated in Figure 2, which is a simplified two-dimensional schematic view of charge distribution among three electrodes. It has been extensively reported in previous reports that direct contact with water will generate a negative triboelectric charge on the PTFE surface (Figure 2a).^{10,18–21} It is assumed that the triboelectric charge is uniformly distributed. As the water front rises and partially covers the region on top of electrode A (Figure 2b), the electric potential of electrode A increases because the negative triboelectric charge is screened by positive ions in the water, which produces transient electron flow away from electrode A (Figure 2b). As a consequence, a net induced charge of positive sign appears on electrodes B and C. Further propagation of the water front will alter the distribution of the induced charge on the three electrodes (Figure 2c–e). The change of induced charge density on these electrodes is quantitatively shown in Figure 2f. Electrodes A and B only possess negative and positive induced charge, respectively, while the sign of induced charge on electrode C is reversed as the water front propagates midway. No matter how the charge

distribution varies, the induced current in the external circuit always flows from the anode to the cathode due to the use of rectifying bridges, generating a single current peak. When the water front recedes, the hydrophobic solid surface will repel water and expose the negative triboelectric charge. Based on similar reasoning, the receding process will produce another current peak.

The electric performance of the TF-TEG was investigated by using an electrometer (Keithley 6514). For a TF-TEG that has a total of 11 electrodes and 10 rectifying bridges, a periodic pulsed voltage at a frequency of 1.25 Hz was obtained on the open-circuit condition, as shown in Figure 3a. The submerging process corresponds to a narrow peak with a high amplitude, while the emerging process corresponds to a wider and smaller voltage peak (inset of Figure 3a). The pulsed voltage is different from the square-shaped signal in previous reports.^{11,22} This is because the measured voltage of the TF-TEG here is essentially the voltage applied onto a reverse-biased diode that is considered as the load in this case. Since the resistance of a diode when reversely biased is very large, high voltage up to 230 V can be achieved (Figure 3a). On the short-circuit condition, a pulsed current of $13 \mu\text{A}$ in amplitude was obtained (Figure 3b). Since the submerging process is faster than the emerging process, it corresponds to a sharper but narrower current peak, as shown in the inset of Figure 3b. As the load resistance increases over $105 \text{ M}\Omega$, the voltage amplitude starts to rise while the current amplitude drops (Figure 3c). Correspondingly, their product, the peak output power, reaches a maximum value of 1.1 mW at an optimal load of $25 \text{ M}\Omega$ (Figure 3d), which presents a 10-fold enhancement

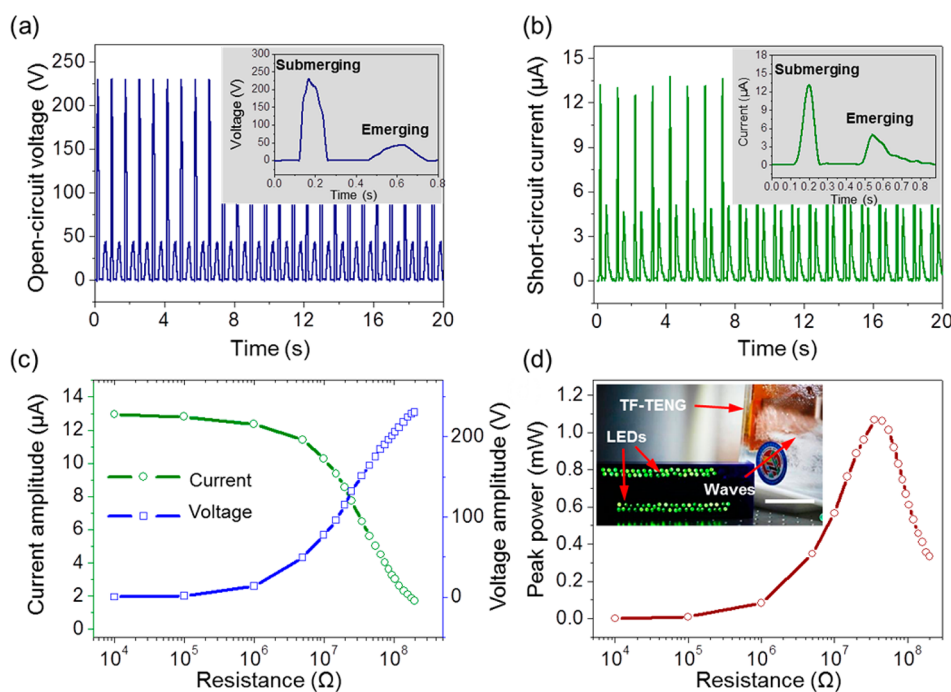


Figure 3. Electric output results of the TF-TEG. (a) Open-circuit voltage (inset: voltage of a single submerging–emerging cycle). (b) Short-circuit current (inset: current of a single submerging–emerging cycle). (c) Current amplitude and voltage amplitude as a function of load resistance. (d) Peak output power as a function of load resistance (inset: picture of powering tens of LEDs by a TF-TEG in a simultaneous way; scale bar = 60 mm).

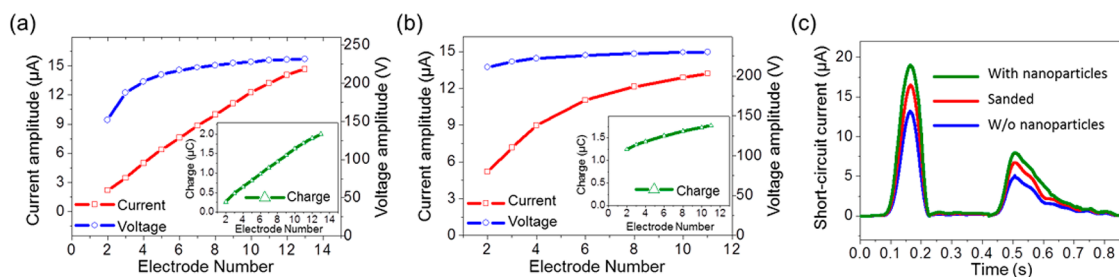


Figure 4. Electric output of the TF-TEG that is affected by internal structural design. (a) Current amplitude and voltage amplitude as a function of the electrode number (inset: induced charge generated in a single submerging–emerging process). (b) Current amplitude and voltage amplitude as a function of the electrode density (inset: induced charge generated in a single submerging–emerging process). (c) Short-circuit current as affected by surface roughness.

over the previous report.¹¹ The TF-TEG can directly power a number of small electronics. Tens of light-emitting diodes (LEDs) are simultaneously powered, as displayed in the inset of Figure 3d and movie S1.

Factors that can influence the electric performance of the TF-TEG are discussed comprehensively. From the aspect of structural design, three factors are investigated. First, increasing the number of electrodes (from 2 to 13) while maintaining the dimensions of each electrode can considerably promote the electric output of the TF-TEG (Figure 4a). The enhancement is attributed to a larger device that has more contact area with water. It is intuitive that the current amplitude as well as the charge quantity carried by a single current peak (inset of Figure 4a) scales linearly in proportion to the number of electrodes because of the area-dependent triboelectric charge. However, the voltage amplitude starts to saturate when the electrode

number is more than 6. This is likely attributed to breakdown of the diodes, which prevents the voltage from further building up. Second, the density of electrodes also plays a role in tuning the electric output. As the number of electrodes increases while the overall area remains constant, more induced charge can flow in the external circuit.²³ As a result, the electric output is promoted (Figure 4b). Besides, surface morphology of the electrification layer is another important factor because it directly relates to the effective contact area at the solid/liquid interface. When compared to a control device that has a smooth surface, TF-TEGs that are modified by sandpapers (Figure S1) and by nanoparticles exhibit enhancements by 24.8 and 44.1% in current amplitude, respectively (Figure 4c).

From the aspect of the external condition, two factors are discussed in this work. First, how fast the

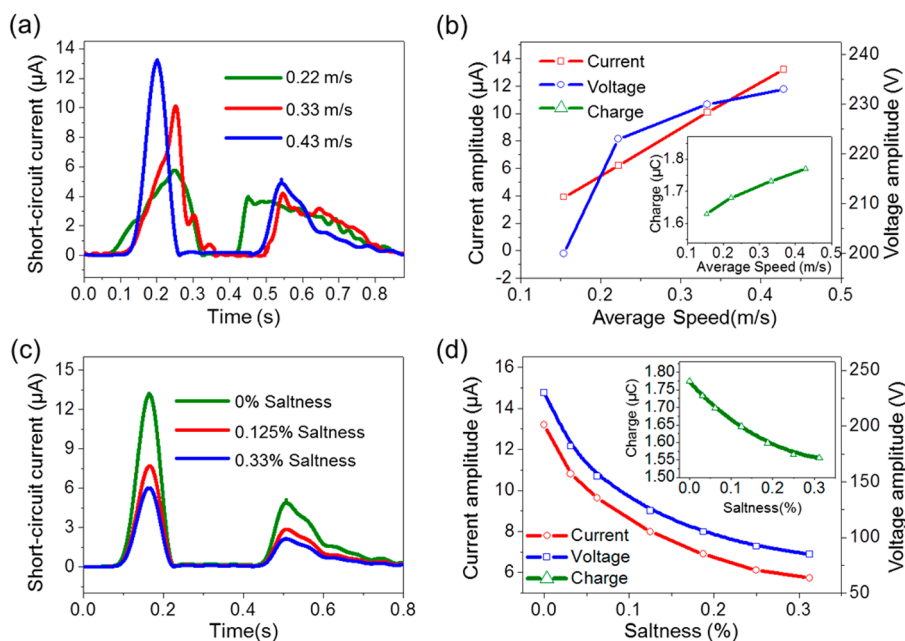


Figure 5. Electric output of the TF-TEG that is affected by external factors. (a) Short-circuit current as influenced by the propagating speed of the water wave. (b) Current amplitude and voltage amplitude as a function of the propagating speed (inset: induced charge generated in a single submerging–emerging process). (c) Short-circuit current as influenced by water saltiness. (d) Current amplitude and voltage amplitude as a function of the water saltiness (inset: induced charge generated in a single submerging–emerging process).

water interacts with the TF-TEG greatly affects the electric output. As demonstrated in Figure 5a, as the average propagation speed of the wave increases, the current peak becomes increasingly sharper and narrower. The larger current amplitude is attributed not only to faster charge flow but also to higher quantity of induced charge. This is because more dynamic interaction at the solid/liquid interface generates higher density of triboelectric charge, which has been reported in the literature.^{4,24} Second, the conductivity of water is also noteworthy in affecting the electric output. As the conductivity of water increases, its ability to generate triboelectric charge with a solid surface is weakened.^{10,11} Consequently, salted water will lower the electric output (Figure 5c,d). However, even for saturated salted water, the voltage as well as the current reduces to 40% and still maintains decent values, which is indicative of potential application of the TF-TEG in practical circumstances, such as in rivers and oceans. After 60 h of continuous testing at a wave frequency of 2 Hz, the nanoparticles still fully cover the PTFE surface with unchanged surface morphology (Figure S2). The average thickness only reduced by about 9 nm, which indicates good durability of the surface modification.

The produced electricity can become a power source for a variety of purposes. Here, we used it for impressed current cathodic protection of metal. A carbon steel sample was directly connected to the cathode of a TF-TEG and immersed in 0.5 M NaCl solution (Figure 6a). The open-circuit potential (OCP) of the carbon steel stays at -111 mV without protection. When electricity

is fed from the TF-TEG that converts wave energy, the OCP exhibits a considerable negative shift. It takes around 240 s before the OCP becomes stable. After the TF-TEG is removed, the OCP then responds and recovers. Repeated application of the electricity from the TF-TEG results in periodic change of the OCP in a highly repeatable way (Figure 6b). The most negative OCP reaches -198 mV, which shifts by 87 mV compared to the original value. The protection effect can be clearly visualized by the change of surface morphology. As shown in Figure 6c, very little rust marks can be spotted on the sample after 8 h if nonstop protection is applied. After 24 h, traces of observable rust can be found. In contrast, for a control sample without the protection, a thick layer of rust appears and accumulates as time passes (Figure 6d). After 4 h, severe corrosion can be observed, which proves the effectiveness of the protection.

CONCLUSION

In summary, we reported a flexible thin-film triboelectric generator for harvesting kinetic wave energy. It is the triboelectric charge at the solid/liquid interface that induces electron flow in the external circuit. An area-scalable integration approach was developed by using an array of surface-mounted bridge rectifiers, which ensured constructive addition of output current from all electrodes to form pulsed direct current. Besides, surface modification by spin-coated nanoparticles can be achieved in a large area. As a result, the TF-TEG has the potential to be scaled up in area. The produced electricity not only drove small

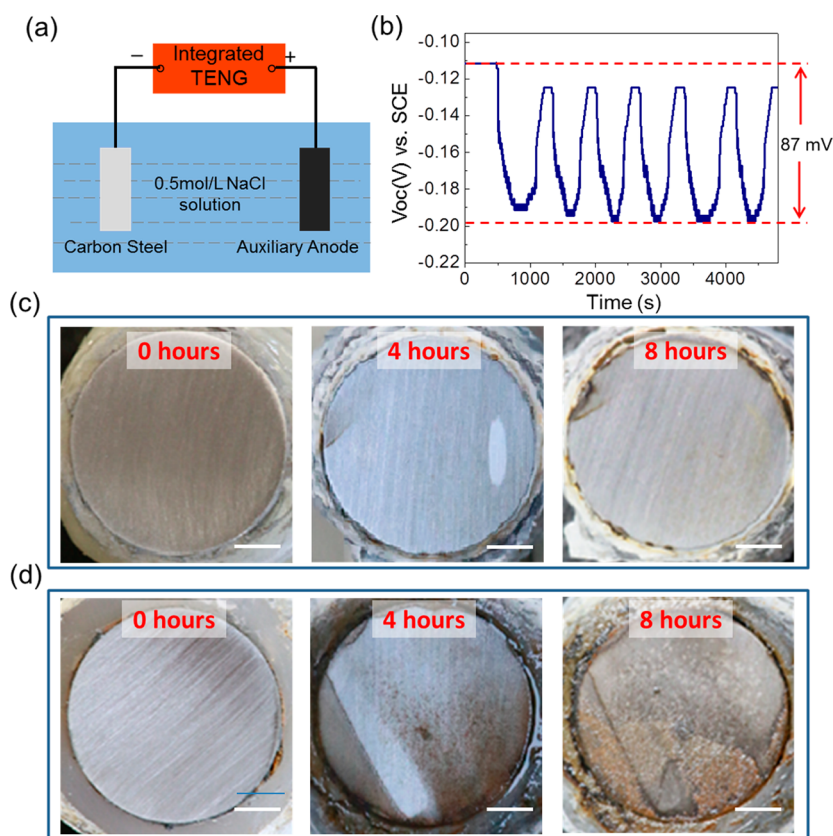


Figure 6. Impressed current cathodic protection for carbon steel by the TF-TEG. (a) Experimental setup for the cathodic protection. (b) Open-circuit potential of the carbon steel varies in a repeated way as the electricity from the TF-TEG is periodically applied. (c) Surface morphology change of the carbon steel if the corrosion protection is applied (scale bars = 15 mm). (d) Surface morphology change of the carbon steel without the protection (scale bars = 15 mm).

electronics but also enabled effective impressed current cathodic protection for carbon steel. Therefore, the TF-TEG is a potentially practical solution of on-site

sustained power supply, especially suitable for corrosion protection at either coastal or off-shore sites wherever wave energy is available.

METHODS

Fabrication of a TF-TEG. A Kapton film of 125 μm in thickness was selected. Then two sets of masks were prepared by a laser cutting machine. The first set defines the electrode array and the comb-shaped joint cathode, which were deposited by sputtering a layer of copper (200 nm thick) at a deposition rate of 0.1 nm/s. The second set of masks defines the anode. Before the anode was deposited, an insulating layer of parylene (3 μm thick) was deposited onto the premade cathode. Once the anode was deposited (200 nm of copper by sputtering), the positions of the bridge rectifiers became well-defined. They were then fixed onto the electrodes using conductive silver epoxy. Finally, PTFE thin film that had adhesive on one side was applied on top of the device.

Surface Modification of PTFE Film. Here we adopted two methods to introduce surface roughness that can increase the effective contact area with water. One method is to sand the PTFE film surface with fine grit sandpaper (2000#). The sanding was applied horizontally as well as vertically, which forms a rectangular mesh surface texture in microscopic scale. The second method is spin-coating PTFE nanoparticles to form a bumpy surface at the nanoscale. PTFE resin that consists of PTFE nanoparticles (6%) and water was applied. It was spun at 1000 rpm for 60 s on the PTFE surface that was pretreated with O_2/Ar plasma for 60 s. Then it was dried in a vacuum oven at 150 $^\circ\text{C}$ for 1 h. The thickness of the close-packed nanoparticle layer was around 1 μm .

Conflict of Interest: The authors declare no competing financial interest.

Supporting Information Available: Additional figures. The Supporting Information is available free of charge on the ACS Publications website at DOI: 10.1021/acsnano.5b03093.

Acknowledgment. The research was supported by the “thousands talents” program for pioneer researcher and his innovation team in China. Patents have been filed based on the research presented here.

REFERENCES AND NOTES

- Muetze, A.; Vining, J. G. *Ocean Wave Energy Conversion - A Survey*. 41st Industry Applications Society Annual Meeting; Tampa, FL, October 8–12, **2006**.
- Sabzehgar, R.; Moallem, M. A Review of Ocean Wave Energy Conversion Systems. *Electrical Power & Energy Conference (EPEC)*; Montreal, QC, October 22–23, **2009**; DOI: 10.1109/EPEC.2009.5420927.
- Khaligh, A.; Onar, O. C. *Energy Harvesting: Solar, Wind, and Ocean Energy Conversion Systems*; CRC Press: Boca Raton, FL, 2009.
- Lin, Z.-H.; Cheng, G.; Wu, W.; Pradel, K. C.; Wang, Z. L. Dual-Mode Triboelectric Nanogenerator for Harvesting Water

- Energy and As a Self-Powered Ethanol Nanosensor. *ACS Nano* **2014**, *8*, 6440–6448.
- Murray, R.; Rastegar, J. Novel Two-Stage Piezoelectric-Based Ocean Wave Energy Harvesters for Moored or Unmoored Buoys. *Proc. SPIE* **2009**, *7288*, 72880E(1)–72880E(12).
 - Scruggs, J.; Jacob, P. Harvesting Ocean Wave Energy. *Science* **2009**, *323*, 1176–1178.
 - Kornbluh, R. D.; Pelrine, R.; Prahlaad, H.; Wong-Foy, A.; McCoy, B.; Kim, S.; Eckerle, J.; Low, T. From Boots to Buoys: Promises and Challenges of Dielectric Elastomer Energy Harvesting. *Proc. SPIE* **2011**, *7976*, 797605(1)–797605(19).
 - Drouen, L.; Charpentier, J. F.; Semail, E.; Clenet, S. Study of an Innovative Electrical Machine Fitted to Marine Current Turbines. *Proc. Oceans 2007–Eur.*; Aberdeen, June 18–21, **2007**; pp 1–6.
 - Wang, Z. L. Triboelectric Nanogenerators As New Energy Technology for Self-Powered Systems and As Active Mechanical and Chemical Sensors. *ACS Nano* **2013**, *7*, 9533–9557.
 - Lin, Z. H.; Cheng, G.; Lin, L.; Lee, S.; Wang, Z. L. Water-Solid Surface Contact Electrification and Its Use for Harvesting Liquid Wave Energy. *Angew. Chem., Int. Ed.* **2013**, *52*, 12545–12549.
 - Zhu, G.; Su, Y.; Bai, P.; Chen, J.; Jing, Q.; Yang, W.; Wang, Z. L. Harvesting Water Wave Energy by Asymmetric Screening of Electrostatic Charges on a Nanostructured Hydrophobic Thin-Film Surface. *ACS Nano* **2014**, *8*, 6031–6037.
 - Guigon, R.; Chaillout, J.-J.; Jager, T.; Despesse, G. Harvesting Raindrop Energy: Experimental Study. *Smart Mater. Struct.* **2008**, *17*, 015039.
 - Ma, M.; Guo, L.; Anderson, D. G.; Langer, R. Bio-Inspired Polymer Composite Actuator and Generator Driven by Water Gradients. *Science* **2013**, *339*, 186–189.
 - Kwon, S.-H.; Park, J.; Kim, W. K.; Yang, Y.; Lee, E.; Han, C. J.; Park, S. Y.; Lee, J.; Kim, Y. S. An Effective Energy Harvesting Method from a Natural Water Motion Active Transducer. *Energy Environ. Sci.* **2014**, *7*, 3279–3283.
 - Chen, J.; Yang, J.; Li, Z.; Fan, X.; Zi, Y.; Jing, Q.; Guo, H.; Wen, Z.; Pradel, K. C.; Niu, S.; et al. Networks of Triboelectric Nanogenerators for Harvesting Water Wave Energy: A Potential Approach toward Blue Energy. *ACS Nano* **2015**, *9*, 3324–3331.
 - Guo, W.; Li, X.; Chen, M.; Xu, L.; Dong, L.; Cao, X.; Tang, W.; Zhu, J.; Lin, C.; Pan, C.; Wang, Z. L. Electrochemical Cathodic Protection Powered by Triboelectric Nanogenerator. *Adv. Funct. Mater.* **2014**, *24*, 6691–6699.
 - Henderson, R. Design, Simulation, And Testing Of A Novel Hydraulic Power Take-Off System For The Pelamis Wave Energy Converter. *Renewable Energy* **2006**, *31*, 271–283.
 - Ravelo, B.; Duval, F.; Kane, S.; Nsom, B. Demonstration of the Triboelectricity Effect by the Flow of Liquid Water in the Insulating Pipe. *J. Electrostat.* **2011**, *69*, 473–478.
 - Choi, D.; Lee, H.; Im, I. J.; Kang, I. S.; Lim, G.; Kim, D. S.; Kang, K. H. Spontaneous Electrical Charging of Droplets by Conventional Pipetting. *Sci. Rep.* **2013**, *3*, 2037.
 - Huang, W.; Wang, G.; Gao, F.; Qiao, Z.; Wang, G.; Chen, M.; Deng, Y.; Tao, L.; Zhao, Y.; Fan, X.; et al. Energy Harvesting from the Mixture of Water and Ethanol Flowing through Three-Dimensional Graphene Foam. *J. Phys. Chem. C* **2014**, *118*, 8783–8787.
 - Yatsuzuka, K.; Mizuno, Y.; Asano, K. Electrification Phenomena of Pure Water Droplets Dripping and Sliding on a Polymer Surface. *J. Electrostat.* **1994**, *32*, 157–171.
 - Jeong, C. K.; Baek, K. M.; Niu, S.; Nam, T. W.; Hur, Y. H.; Park, D. Y.; Hwang, G.-T.; Byun, M.; Wang, Z. L.; Jung, Y. S.; et al. Topographically-Designed Triboelectric Nanogenerator via Block Copolymer Self-Assembly. *Nano Lett.* **2014**, *14*, 7031–7038.
 - Niu, S.; Wang, S.; Liu, Y.; Zhou, Y. S.; Lin, L.; Hu, Y.; Pradel, K. C.; Wang, Z. L. A Theoretical Study of Grating Structured Triboelectric Nanogenerators. *Energy Environ. Sci.* **2014**, *7*, 2339–2349.
 - Leng, Q.; Guo, H.; He, X.; Liu, G.; Kang, Y.; Hu, C.; Xi, Y. Flexible Interdigital-Electrodes-Based Triboelectric Generators for Harvesting Sliding and Rotating Mechanical Energy. *J. Mater. Chem. A* **2014**, *2*, 19427–19434.